

Interactive artificial ecosystem algorithm for solving power management optimizations

Introduction. Power planning and management of practical power systems considering the integration and coordination of various FACTS devices is a vital research area. Recently, several metaheuristic methods have been developed and applied to solve various optimization problems. Among these methods, an artificial ecosystem based optimization has been successfully proposed and applied to solve various industrial and planning problems. **The novelty** of the work consists in creating an interactive process search between diversification and intensification within the standard artificial ecosystem based optimization. The concept of the introduced variant is based on creating dynamic interaction between production operator and consumer operator during search process. **Purpose.** This paper introduces an interactive artificial ecosystem based optimization to solve with accuracy the multi objective power management optimization problems. **Methods.** The solution of the problem was carried out using MATLAB program and the developed package is based on combining the proposed metaheuristic method and the power flow tool based Newton-Raphson algorithm. **Results.** Obtained results confirmed that the proposed optimizer tool may be suitable to solve individually and simultaneously various objective functions such as the total fuel cost, the power losses and the voltage deviation. **Practical value.** The efficiency of the proposed variant in terms of solution quality and convergence behavior has been validated on two practical electric test systems: the IEEE-30-bus, and the IEEE-57-bus. A statistical comparative study with critical review is elaborated and intensively compared to various recent metaheuristic techniques confirm the competitive aspect and particularity of the proposed optimizer tool in solving with accuracy the power management considering various objective functions. References 34, tables 11, figures 16.

Key words: artificial ecosystem based optimization, power management, intensification and diversification, FACTS devices.

Вступ. Планування електроживлення та управління енергосистемами, що експлуатуються, з урахуванням інтеграції та координації різних пристроїв FACTS (гнучка система передачі змінного струму) є життєво важливою галуззю досліджень. Останнім часом було розроблено та застосовано кілька метаевристичних методів для вирішення різних задач оптимізації. Серед цих методів оптимізація на основі штучної екосистеми була успішно запропонована та застосована для вирішення різних промислових та планувальних завдань. **Новизна** роботи полягає у створенні інтерактивного процесу пошуку між диверсифікацією та інтенсифікацією в рамках стандартної оптимізації на основі штучної екосистеми. Концепція представленого варіанта заснована на створенні динамічної взаємодії між оператором-виробником та оператором-споживачем у процесі пошуку. **Мета.** У статті представлено інтерактивну оптимізацію на основі штучної екосистеми для точного вирішення базатоцільових завдань оптимізації управління живленням. **Методи.** Розв'язання задачі здійснювалося за допомогою програми MATLAB, а розроблений пакет заснований на об'єднанні запропонованого метаевристичного методу та інструменту Powerflow на основі алгоритму Ньютона-Рафсона. **Результати.** Отримані результати підтвердили, що запропонований інструмент оптимізатора може бути придатний для індивідуального та одночасного розв'язання різних цільових функцій, таких як загальна вартість палива, втрати потужності та відхилення напруги. **Практична цінність.** Ефективність запропонованого варіанта з точки зору якості рішення та поведінки збіжності була підтверджена на двох реальних електричних випробувальних системах: шині IEEE-30 та шині IEEE-57. Статистичне порівняльне дослідження з критичним оглядом розроблено та інтенсивно порівнюється з різними сучасними метаевристичними методами, що підтверджують конкурентний аспект та особливість запропонованого інструменту оптимізатора у точному розв'язанні управління живленням з урахуванням різних цільових функцій. Бібл. 34, табл. 11, рис. 16.

Ключові слова: оптимізація на основі штучної екосистеми, управління енергією, інтенсифікація та диверсифікація, пристрої FACTS (гнучка система передачі змінного струму).

Introduction. As well demonstrated and stated in many research papers, that no a standard optimizer tool capable to solve various optimization tasks. For this reason, many optimizer tools based metaheuristic algorithms known also as global optimization methods have been developed. It is well proven that each developed method has its specific drawbacks and advantages, so, the majority of metaheuristic methods have special parameters to adjust designed to balance the search activity between intensification and diversification. The famous idea firstly introduced by Carpentier [1] namely economic dispatch which is a simplified and particular case of optimal power flow (OPF) becomes a vital tool for solving various power management optimization problems. The OPF planning strategy consists in improving the solution quality of a single or combined objective functions such as the total fuel cost (TFC), the total power loss (TPL), the total voltage deviation (TVD) and the voltage stability (VS) index while satisfying various security constraints. The concept of OPF tool becomes more attractive and vital for experts with the intensive installation of several types of flexible ac transmission system (FACTS) and the intense

orientation towards integration of renewable sources. In the literature various determinist methods based mathematical formulation and several metaheuristic techniques have been proposed to solve many power management problems associated to modern electric systems. These methods have been designed and adapted to solve the conventional single or multi objective OPF considering several FACTS and various renewable sources energy such as wind and photovoltaic sources. In [2] a brief review is proposed on the famous metaheuristic methods applied to solve various power systems planning and control, among these methods: Genetic algorithm (GA), particle swarm optimization (PSO), differential evolution (DE), tabu search algorithm (TS), simulated annealing, etc. Continuously and to enhance the performances of the standard metaheuristic algorithms, many variants have been developed. The main idea introduced by these variants based metaheuristic methods such as in [3] are focused on how adjusting with efficacy the evolution of specific parameters and how to create flexible equilibrium during search process between diversification and intensification. Towards this pertinent

context, and to improve the solution of various practical configurations associated to the multi objective OPF, various recent optimization techniques have been designed and proposed. These recent optimization techniques characterized by low parameters to adjust, and their research mechanism is adaptive to create a flexible balance during search process between intensification and diversification. Among these methods, in [4] authors proposed a new interactive sine cosine algorithm (ISCA) to solve the security OPF considering critical state operations. In the same context, an interactive procedure named micro SCA is introduced and greatly improved the mechanism search of the standard SCA. In [5] a new variant named partitioning whale algorithm (PWOA) has been successfully applied to solve with accuracy the multi objective OPF. In [6] a new chaotic electromagnetic field algorithm based optimization is applied to improve the solution of the OPF. In [7] authors applied a moth swarm optimizer (MSO) to solve the OPF considering various operation and security constraints. In [8] an enhanced grasshopper variant is adapted and used to solve the multi objective OPF. In [9] authors suggested a variant based Jaya algorithm (AMTPG-Jaya) to enhance the solution of multi objective OPF. In [10] a new algorithm named tree seed algorithm (TSA) is proposed. In [11] a hybrid algorithm based on combing the PSO and gravitational search algorithm (GSA) is proposed to enhance the solution of the multi objective OPF. In [12] the lightning attachment optimization (LAO) technique is used for solving the security OPF. In [13] a combined technique based on PSO and pattern search (PS) algorithm is adapted to solve the OPF considering the integration of FACTS controllers. In [14] a variant based on teaching-learning algorithm is applied to solve the multi objective OPF. In [15] a chaotic bat algorithm (CBA) is adapted and applied to solve the reactive power management (RPM) problems. In [16] a new variant based social spider optimization (SSO) algorithm is used to improve the performances of the standard algorithm in solving the OPF by considering various goal functions. In [17] the PSO, GA and evolutionary algorithm (EA) are applied to solve the multi objective OPF problems. In [18] a new adaptive partitioning flower pollination algorithm (APFPA) is introduced and successfully applied to improve the OPF solution considering various objective functions at normal condition and under load growth. In [19] a modified salp swarm algorithm (MSSA) is successfully adapted and applied to solve the reactive power management optimization of the Algerian electric power system. In [20], a chaotic salp swarm algorithm (CSSA) is applied to solve various objective functions based OPF. In [21] a new stud krill herd algorithm (SKH) is adapted and used to solve the OPF with various objective functions. In [22] an improved adaptive differential evolution is suggested to solve various objectives based OPF problems. In [23] a novel variant based salp swarm algorithm is successfully applied to improve the solution quality of the multi objective OPF. In [24] a squirrel search algorithm is applied to solve the economic dispatch considering practical constraints such as the valve loading effect and multiple fuels. In [25] a novel variant based grey wolf optimizer (GWO) namely,

crisscross search based GWO (CS-GWO) is proposed to solve the OPF considering several objective functions. In [26] the whale optimizer is adapted and applied to solve the dynamic economic emission dispatch. In [27] a slime mould algorithm is proposed to solve the stochastic optimal power flow based wind energy and considering static VAR compensators. In [28] a hybrid algorithm based on combing the genetic algorithm and the salp swarm algorithm to solve the simultaneous allocation of multiple distribution generation and shunt compensators to improve the performances of radial distribution systems.

Recently, a new optimizer tool based metaheuristic concept namely artificial ecosystem optimizer (AEO) has been proposed by in [29]. AEO is inspired from the interactive flow of energy in an ecosystem on the earth. The robustness of the proposed mechanism search based AEO has been validated on many categories of test benchmark functions and practical engineering problems [29]. In the literature the standard AEO algorithm and a limited number of proposed variants based AEO have been applied to solve various practical optimization problems, however, a very limited number of variants based AEO have been proposed and applied to solve the active and reactive power management optimization problems without considering the integration of FACTS devices. Among these variants based AEO, in [30] the standard AEO is adapted to solve the reactive power management of many electric test systems such as the IEEE 30-Bus, the IEEE 118-Bus, the 300-Bus and the Algerian electric network 114-Bus, in this study, the bank compensators are the main compensator devices investigated to improve the performances of the reactive power management. In [31] the standard AEO is successfully investigated to solve the reconfiguration of radial distribution systems considering the integration of multi distributed generations (DGs) and multi bank capacitors. In [32] the AEO is designed and applied to solve the combined problem based optimal locations of photovoltaic (PV) and wind sources based DGs and compensator devices, and in [33] an enhanced AEO is designed and adapted to solve the optimal location of DGs to minimize the TPL in radial distribution systems. In this study an interactive variant based AEO is proposed to solve various multi objective power management problems considering the integration of multi SVC devices based FACTS technology. The main contributions achieved in this paper compared to the standard AEO and to other metaheuristic techniques are summarized in four points:

- a new variant named interactive AEO is proposed to solve the multi objective power management optimization problems;
- a dynamic interaction between production operator and consumer operator during search process is introduced to right balance between diversification and intensification;
- the proposed interactive artificial ecosystem optimizer (IAEO) is characterized by a flexible equilibrium during search process between intensification and diversification;
- the TFC, the TPL and the TVD are three main objective functions optimized individually and simultaneously;

- the proposed IAEO validated on two standard electric systems (IEEE-30-Bus and IEEE-57-Bus) and an effective comparative study and critical review with many methods have been elaborated to demonstrate the efficiency of the proposed IAEO.

Power management optimization. The task of power management optimization known also as OPF is to minimize one or multi objective functions. The equality $H(X, U) = 0$ and the inequality constraints $G(X, U) \leq 0$ related to operation security of electric systems [5] must be satisfied. The mathematical formulation of the multi objective power management optimization is expressed as follow:

$$\begin{aligned} & \text{Min } \{obj_F_i\} = \\ & = \text{Min } \{obj_F_1, obj_F_2, obj_F_3, \dots, obj_F_{nobj}\} \end{aligned} \quad (1)$$

Subject to:

Power balance constraints: represents the balance of active and reactive power between production and demand

$$H(X, U) = 0 \Leftrightarrow \begin{cases} P_{gi} - P_{di} - V_i \sum_{j=1}^N V_j (g_{ij} \cos \delta_{ij} + b_{ij} \sin \delta_{ij}) = 0 \\ Q_{gi} - Q_{di} - V_i \sum_{j=1}^N V_j (g_{ij} \sin \delta_{ij} - b_{ij} \cos \delta_{ij}) = 0 \end{cases} \quad (2)$$

Operation constraints: reflects technical admissible operation limits of various elements of electric networks

$$G(X, U) \leq 0 \Leftrightarrow \begin{cases} V_{gi}^{\min} \leq V_{gi} \leq V_{gi}^{\max} \\ P_{gi}^{\min} \leq P_{gi} \leq P_{gi}^{\max} \\ Q_{gi}^{\min} \leq Q_{gi} \leq Q_{gi}^{\max} \\ T_i^{\min} \leq T_i \leq T_i^{\max} \\ Q_{svci}^{\min} \leq Q_{svci} \leq Q_{svci}^{\max} \\ V_{Li}^{\min} \leq V_{Li} \leq V_{Li}^{\max} \\ S_{li} \leq S_{li}^{\max} \end{cases} \quad (3)$$

The vectors X and U are expressed as:

$$X^T = [\delta, V_L(1 \dots N_{PQ}), P_{gs}, Q_g(1 \dots N_{PV})]; \quad (4)$$

$$U^T = [P_g(1 \dots N_{PV}), V_g(1 \dots N_{PV}), Q_{svc}(1 \dots N_{svc}), T(1 \dots N_T)]. \quad (5)$$

Various objective functions.

TFC minimization. The objective function associated to the TFC is expressed as follows.

$$OBJ_1(X, U) = \min(TFC) = \min \left(\sum_{i=1}^{NG} (a_i + b_i P_{gi} + c_i P_{gi}^2) \right), \quad (6)$$

where NG is the number of thermal generating units; P_{gi} is the real power of the i th generator; a_i , b_i , and c_i are the cost coefficients of the i th generator.

TVD minimization. The objective function associated to the TVD is expressed as:

$$OBJ_2(X, U) = \min(TVD) = \min \left(\sum_{i \in NL} |V_i - V_{des}| \right), \quad (7)$$

where V_{des} is the desired voltage magnitudes at all load buses.

TPL minimization. The objective function associated to the TPL is formulated as follow:

$$\begin{aligned} OBJ_3(X, U) &= \min(TPL) = \\ &= \min \left(\sum_{k=1}^{N_l} g_k \left[(t_k V_i)^2 + V_j^2 - 2t_k V_i V_j \cos \delta_{ij} \right] \right). \end{aligned} \quad (8)$$

TFC minimization in coordination with TVD. The objective function based on combining the TFC and the TVD is modelled using the following equation.

$$OBJ_4(X, U) = \text{Min} \left(\left(\sum_{i=1}^{NG} (a_i + b_i P_{gi} + c_i P_{gi}^2) \right) + \beta(TVD) \right), \quad (9)$$

where β is a balancing factor.

Constraints management. Modified objective function is formulated using the following expression [18]:

$$OBJ_{\text{mod}}(X, U) = OBJ_i(X, U) + Pen; \quad (10)$$

$$\begin{aligned} Pen &= \gamma_v \times \sum_{i=1}^{N_{PQ}} (V_{Li} - V_{Li}^{\text{lim}})^2 + \gamma_Q \times \sum_{i=1}^{N_{PV}} (Q_{gi} - Q_{gi}^{\text{lim}})^2 + \\ &+ \gamma_{P_s} \times (P_{gs} - P_{gs}^{\text{lim}})^2 + \gamma_{br} \times \sum_{i=1}^{N_l} (S_{bri} - S_{bri}^{\text{lim}})^2, \end{aligned} \quad (11)$$

where γ_v , γ_Q , γ_{P_s} and γ_{br} are the penalty coefficients related to state variables [5].

Static Var Compensator (SVC) model. The SVC device is one of shunt compensators from the family of FACTS. As well shown in Fig. 1, the principle of SVC device consists in controlling the voltage magnitude at specified bus absorbing or injecting reactive power. The expression of reactive power Q_i^{SVC} controlled by the SVC device is given as follow:

$$Q_i^{SVC} = -B_{SVC} \cdot V_i^2. \quad (12)$$

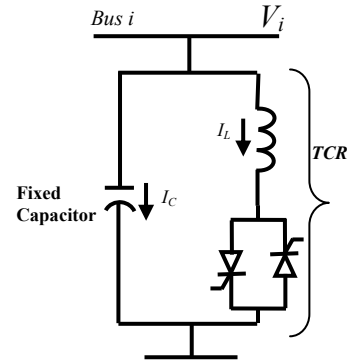


Fig. 1. Basic structure of the SVC

Basic structure of AEO. Recently in [29], authors developed a new optimizer tool based on ecosystem concept namely AEO. The standard AEO mimics the behavior of energy flow in an ecosystem. The basic architecture of the standard AEO is shown in Fig. 2, and the key steps of the AEO are described in the following:

- the main structure of AEO consists of three interactive operators organized based on their energy level;
- in the population, there is only one operator named the Producer which represents the plants in nature. Only one decomposer operator which is known as bacteria and fungi, and the remaining of individuals in the population are designed as consumers known in nature as animals selected as carnivores, herbivores or omnivores;

- the fitness function designed to evaluate all individuals is based on the level of their energy. High level of energy indicates that the selected individual will be the best candidate solution;
- the main task of the producer operator is dedicated to create balance between exploration and exploitation; however the consumer operators are oriented to execute intensification in coordination with the decomposer operator at specified iterations.

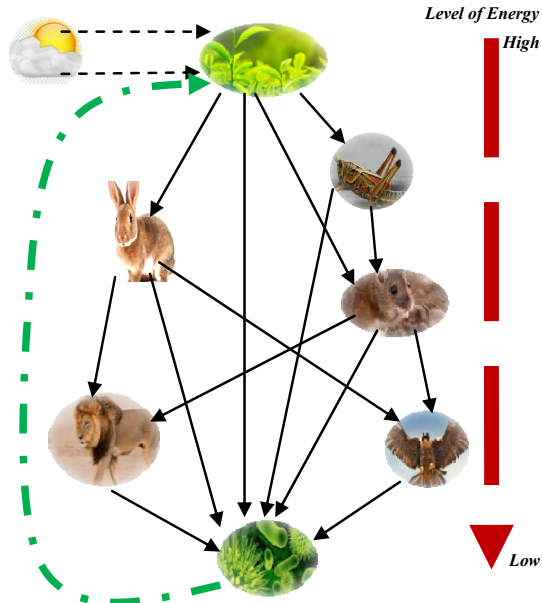


Fig. 2. Basic structure of an ecosystem

Mathematical modeling of AEO. Based on the flowchart shown in Fig. 3, the operators of the standard AEO are described as follows.

Production operator: based on the original AEO [29], the task of the producer operator in an ecosystem is to generate food energy. The evolution of production operator is modeled using the following mathematical expressions:

$$X_1(it+1) = (1-a) \times X_n(it) + a \times X_{rand}(it); \quad (13)$$

$$a = (1-it/T_{max}) \cdot r_1; \quad (14)$$

$$X_{rand} = r \cdot (U_{max} - U_{min}) + U_{min}, \quad (15)$$

where it is the current iteration; X_n is the better candidate found so far; T_{max} is the maximum number of iterations; U_{max} and U_{min} are the maximum and the minimum limits of control variables, respectively; r_1 and r are two random number within the limits $[0, 1]$; a is the linear weight factor; X_{rand} is the random position of an individual.

Consumer operator: The consumers operations are modeled as follows.

For herbivore individuals, the evolution of a random consumer in the search space is modeled using the following equation:

$$X_i(it+1) = X_i(it) + CF \times (X_i(it) - X_1(it)), \quad i \in \{2, \dots, n\}, \quad (16)$$

where CF is a consumption factor defined as follows:

$$CF = \frac{1}{2} \cdot \frac{v_1}{|v_2|}; \quad (17)$$

$$v_1 \sim N(0,1), \quad v_2 \sim N(0,1). \quad (18)$$

For carnivore individuals, mathematically, the behavior of the evolution of carnivores on the search space is modeled as follows:

$$\begin{cases} X_i(it+1) = X_i(it) + CF \times (X_i(it) - X_j(it)), & i \in \{3, \dots, n\}; \\ j = RANDi([2i-1]). \end{cases} \quad (19)$$

For omnivore individuals, it is can each both randomly a consumer with the higher energy level and a producer. The behavior of an omnivore consumer is modeled as follows:

$$\begin{cases} X_i(it+1) = X_i(it) + CF \times (r_2 \times (X_i(it) - X_1(it))); \\ + (1-r_2) \times (X_i(it) - X_j(it)), & i = 3, \dots, n; \\ j = RANDi([2i-1]). \end{cases} \quad (20)$$

Decomposer operator: The equation describing the decomposition behavior is expressed as follows:

$$\begin{cases} X_i(it+1) = X_n(it) + D \times (E \times X_n(it) - H \times X_i(it)), \\ i = 1, \dots, n; \end{cases} \quad (21)$$

$$D = 3 \times u, \quad u \sim N(0,1); \quad (22)$$

$$E = r_3 \times RANDi([1 \ 2]) - 1; \quad (23)$$

$$H = 2 \times r_3 - 1, \quad (24)$$

where D is the decomposition factor; E and H are the weight coefficients; u is the normal distribution with the mean = 0 and the standard deviation = 1.

Algorithm 1: Pseudo code of the standard AEO [29]

```

1  Input setting variables of AEO: Pop_size, Iter_max,
   Trial_max, Dim, ub, lb
2  Generating a population randomly  $X_i$  (solutions),
   evaluate the fitness  $Fit_i$ , and select the best solution
   found so far  $X_{best}$ 
3  While Iter_max and Trial_max not reached do
   //Production operator //
4  For individual  $X_1$ , update its solution using eq. 13
   //Consumption operator //
5  For each individual  $X_i$  ( $i=2, \dots, n$ ),
   // Herbivore operator//
6  If rand<1/3 then update its solution using eq.16,
   // Omnivore operator //
7  Else If 1/3< rand< 2/3 then update its solution using
   eq.19,
   // Carnivore operator //
8  Else update its solution using eq. 20,
9  End If.
10 End If.
11 Evaluate the fitness of each individual.
12 Update the best solution achieved so far  $X_{best}$ .
   // Decomposition operator//
13 Update the position of each individual using equation
   (21).
14 Calculate the fitness of each individual.
15 Update the best solution found so far  $X_{best}$ .
16 End While
17 Return  $X_{best}$ 

```

Strategy of the proposed IAEO based optimal power management. The strategy of the proposed IAEO designed for solving various OPF managements is focused to create interactive equilibrium between diversification and intensification.

Exploration phase. Three coordinated subsystems are designed to accomplish the exploration phase. The first subsystem consists of active powers of generating units, the second subsystem consists of voltage magnitudes of generators and the third subsystems contains the decision variables associated to tap transformers. Figure 3 shows the three decision variables associated to the exploration phase.

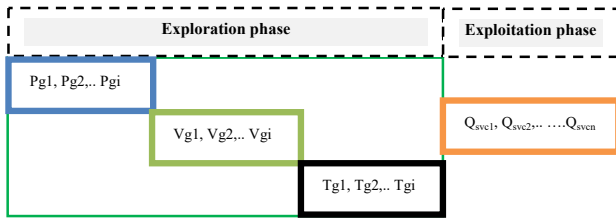


Fig. 3. Decision variables designed for exploration and exploitation phases

The steps of the diversification phase are described as follows.

Stage 1: the task of the first subsystem is designed to optimize only the decision variables associated to active power of generators. The first optimized decision variables achieved during the first stage is identified as Sub1_PG.

Stage 2: the task of the second subsystem is focused to optimize the decision variables related to the voltage magnitudes of thermal generators by considering the Sub1_PG as an initial solution. The second optimized control variables achieved during this stage is named Sub2_VG.

Stage 3: the task of the third subsystem to be optimized is oriented to optimize the decision variables associated to tap transformers by considering Sub1_PG and Sub2_VG as an initial solution. The third optimized control variables found during this third stage is identified as Sub3_T.

Exploitation phase. The task of the intensification phase is to optimize the decision variables associated to reactive power of multi SVC devices by considering the three optimized sub systems such as: Sub1_PG, Sub2_VG, and Sub3_T achieved during the diversification phase.

In this paper, the maximum number of generation and the population size related to this stage are taken 150 and 20 respectively, these values chosen carefully by experience and in general depend on the type of the test system to be solved.

Proposed interactive search process. In the proposed new variant named IAEO, an interactive search process is introduced to improve the solution quality, two modifications are proposed.

The first modification is related to the dynamic evolution of the weight coefficient during search task. The weight factor is controlled during the search process using the following expression:

$$a = (1 - \sin(it/T_{\max})) \times rand \quad (25)$$

The evolution of the weight coefficient for one run is shown in Fig. 4.

The second modification introduced focused on updating the evolution of production operator during search process using the following mathematical expressions:

$$X_1(it+1) = (1-a) \times X_n(it) + a \times X_{rand}(it); \quad (26)$$

$$\begin{aligned} \text{If } It < It_c \quad X_{rand} &= r \times (U_{\max} - U_{\min}) + U_{\min}; \\ \text{if } It > It_c \quad X_{rand} &= r \times (best_Pop_Sol - U_{\min}) + U_{\min}, \end{aligned} \quad (27)$$

where It_c is the critical iteration chosen by experience, it depends on the problem to be solved, in this study, It_c is taken between 10 to 20; $best_Pop_Sol$ is the best solution found so far.

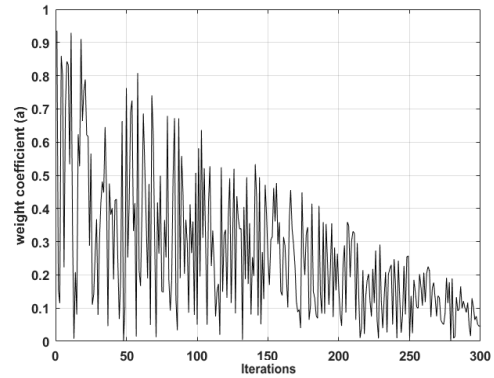


Fig. 4. Evolution of weight coefficient a during search process

Solution steps of the proposed IAEO strategy.

Based on the interactive of the proposed IAEO presented in Fig. 4, the following steps are required to apply the proposed IAEO to solve the OPF with various objective functions:

Step 1: Introduce the data related to eclectic network such as, fuel cost coefficients of generating units, lines and buses technical characteristics, load parameters, and all security and operation limits such as, permissible limits of voltages of generators and PQ-buses, permissible limits of tap transformers, and limits of reactive power of multi SVC.

Step 2: Identify the dimension of all subsystems to be optimized, the sub system for active power generation (Sub1_PG), the sub system for voltage magnitudes of PV bus (Sub2_VG), the sub system for tap transformers (Sub3_TP), and the sub system for reactive power of shunt SVC devices (Sub4_Qsvc).

Step 3: Define parameters of IAEO algorithm associated to each sub system.

Step 4: Execute the exploration phase based IAEO for solving the three subsystems: [Sub1_PG Sub2_VG Sub3_T].

Step 5: Define parameters of the algorithm for the fourth subsystem Sub4_QSVC designed to elaborate the exploitation phase.

Step 6: Elaborate the exploitation phase, and save the new updated global decision variables: [Sub1_PG Sub2_VG Sub3_T Sub4_Qsvc]

Step 7: Repeat all steps until $Trial_{\max}$ is achieved

Cases studies. This section is focused in applying the proposed new variant namely IAEO to optimize various objective functions based OPF management. Two practical test systems are considered to validate the efficiency of the proposed variant. The IEEE-30-bus, and the IEEE-57-bus electric systems. In this study, and for fair comparison with other methods, the initial security limits of SVC devices for the test system IEEE 30-Bus is taken in the limits $[-5, 5]$ MVar, and for IEEE 57-Bus is taken in the limits $[-20, 20]$ MVar. Various objective functions such as, TFC, the TPL and the TVD have been optimized individually and in coordination.

Test-1: IEEE-30-Bus. The standard electric IEEE-30-Bus test system consists of 30 bus and 41 lines, the total load demand to satisfy at normal exploitation is $(283.4+j126)$ MVA. The admissible limits of PQ-buses and PV-buses are in the limits $[0.95, 1.1]$ p.u. The admissible limits of the four tap transformers are in the limits $[0.9, 1.1]$ p.u., nine SVC have been integrated on buses (10, 12, 15, 17, 20, 21, 23, 24, 29), details technical data can be verified in [32]. For this electric network, six

cases have been elaborated to validate the efficacy of the proposed power management optimization based IAEO.

- Case-1: TFC improvement.
- Case-2: TPL improvement.
- Case-3: TVD improvement.
- Case-4: TFC and TPL improvement.
- Case-5: TPL and TVD improvement.
- Case-6: TFC and TVD improvement.

Case-1: TFC improvement. In this case, the proposed algorithm namely IAEO is applied to find the best fuel cost. Four vectors of control variables such as real power and voltages of thermal generators, tap transformers, and shunt compensators based SVC devices have been optimized. In order to create diversity in search space, four vector of decision variables (PG, VG, TP and Qsvc) are optimized based on interactive mechanism search. Figures 5, *a-c* show the convergence characteristics related to the three stages, it is found that the best cost is improved from stage to stage.

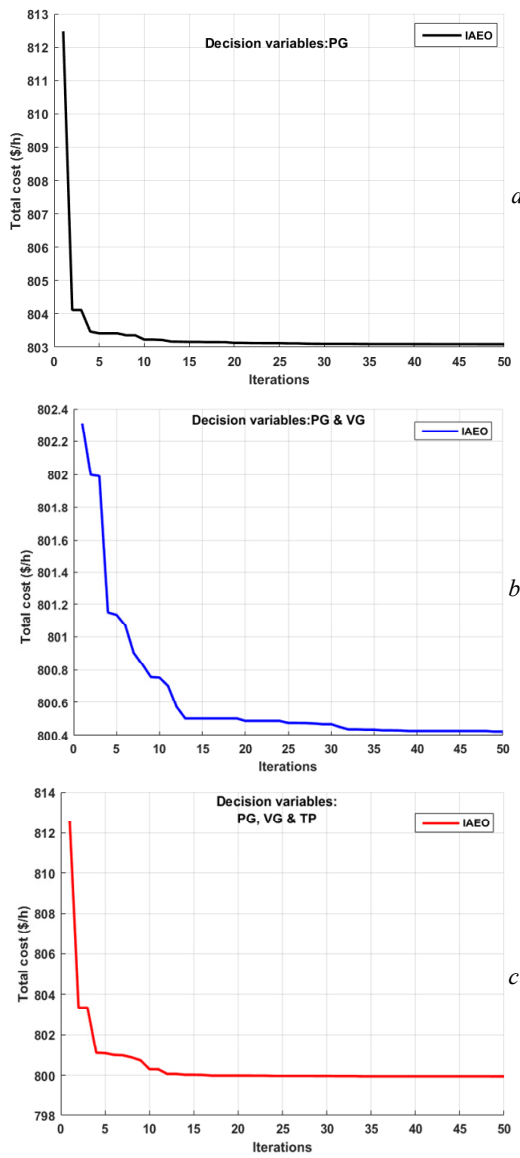


Fig. 5.

- a* – convergence behavior of TFC minimization using IAEO at stage 1 (decision variables PG) for IEEE-30-Bus;
- b* – convergence behavior of TFC minimization using IAEO at stage 2 (decision variables PG and VG) for IEEE-30-Bus;
- c* – convergence behavior of TFC minimization using IAEO at stage 3 (decision variables PG, VG and TP) for IEEE-30-Bus

For this first case, and as well depicted in Table 1, the optimized TFC achieved at the final phase is 798.9457 \$/h, which is better compared to the results found using various recent methods. The convergence behavior of the TFC minimization at the final stage is shown in Fig. 6. The profiles of voltages are shown in Fig. 11. As well shown in Table 2, the proposed IAEO variant outperforms many optimization techniques.

Table 1

The main optimized decision variables for IEEE-30-bus test system

Decision variables	Case-1	Case-2	Case-3	Case-4	Case-5	Case-6
P_{g1}	176.9702	51.2353	143.6338	150.9415	54.1571	165.6028
P_{g2}	48.3087	80.0000	29.6343	53.4670	79.8185	51.4071
P_{g5}	21.2048	50.0000	46.2980	26.2350	49.9782	24.8121
P_{g8}	21.5845	35.0000	27.6480	25.9711	34.5076	23.5360
P_{g11}	11.8614	30.0000	26.4342	16.8140	29.6331	12.3987
P_{g13}	12.0379	40.0000	16.3812	16.8992	38.9481	15.2052
V_{g1}	1.1000	1.0999	1.0125	1.1000	1.0127	1.0127
V_{g2}	1.0876	1.0976	1.0038	1.0876	1.0040	1.0040
V_{g5}	1.0612	1.0799	1.0135	1.0612	1.0137	1.0137
V_{g8}	1.0690	1.0871	1.0020	1.0690	1.0022	1.0022
V_{g11}	1.1000	1.0999	1.0515	1.1000	1.0517	1.0517
V_{g13}	1.1000	1.0999	1.0137	1.1000	1.0139	1.0139
T_{11}	1.0380	1.0438	1.0701	1.0405	1.0729	1.0692
T_{12}	0.9069	0.9142	0.9013	0.9094	0.9041	0.9004
T_{15}	0.9748	0.9813	0.9777	0.9773	0.9805	0.9768
T_{36}	0.9653	0.9707	0.9717	0.9678	0.9745	0.9708
Q_{svc10}	4.8612	4.8518	3.1553	4.5818	3.1955	2.8531
Q_{svc12}	4.7156	3.1956	4.1130	4.2198	4.5578	4.3988
Q_{svc15}	4.9608	2.9111	2.4363	4.9965	2.4236	2.3942
Q_{svc17}	4.8951	4.8909	4.1329	4.0765	4.1939	3.8261
Q_{svc20}	4.2697	3.7933	4.0801	4.3004	4.0587	4.0095
Q_{svc21}	4.9608	4.9008	4.6292	4.9965	4.6050	4.5491
Q_{svc23}	4.1186	2.6759	4.6118	4.1482	4.5876	4.5320
Q_{svc24}	4.5288	4.9008	4.4672	4.2328	4.3305	3.8259
Q_{svc29}	2.7809	2.5299	4.0889	1.8013	4.0675	3.0218
TPL, MW	8.5675	2.835300	6.6294	6.9278	3.6426	9.5619
TFC, \$/h	798.9457	967.0310	860.9828	805.5460	964.2807	807.0926
TVD, p.u.	1.9582	2.0747	0.1098	1.8877	0.1204	0.1348

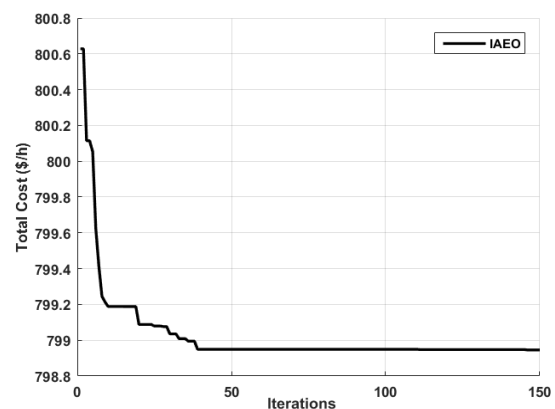


Fig. 6. Convergence behavior for TFC minimization using IAEO at the final stage for IEEE-30-Bus

Table 2

Comparison results of TFC minimization:
test system IEEE-30-Bus:
Voltage of PQ bus limits [0.95, 1.1] (p.u.)

Methods referenced in: [4, 5, 18]	TFC, \$/h	TPL, MW	TVD, p.u.
TLBO	799.0715	–	–
GSA	798.6751*	–	–
DSA	799.0943	–	–
BBO	799.1116	–	–
DE	799.2891	–	–
SA	799.4500	–	–
AGAPOP	799.8441	–	–
BHBO	799.9217	–	–
EM	800.0780	–	–
EADHDE	800.1579	–	–
EADDE	800.2041	–	–
PSO	800.4100	–	–
FPSO	800.7200	–	–
IGA	800.8050	–	–
PSO	800.9600	–	–
GAF	801.2100	–	–
ICA	801.8430	–	–
EGA	802.0600	–	–
TS	802.2900	–	–
MDE	802.3760	–	–
IEP	802.4650	–	–
EP	802.6200	–	–
RGA	804.0200	–	–
GM	804.8530	–	–
GA	805.9400	–	–
GWO	–	2.9377	–
ABC	–	3.0410	–
ICEFO	799.0343	–	–
Proposed IAEO	798.9457	2.8353	0.1098

Case-2: TPL improvement. In this second case, the TPL is considered for optimization. Also, four control decision variables have been optimized in coordination. The TPL has an economic and technical aspect. Network with high losses in lines will affect the reliability of electric system in particular at critical situation. Figures 7,*a-c* show the convergence behavior related to TPL minimization for the three stages. It is found that the best TPL is improved from stage to stage. For this second case, and as well shown in Table 1, the TPL is optimized at a competitive value 2.8353 MW which is better than the result found using standard AEO and also compared to several recent methods. As well depicted in Table 1, and by optimizing the TPL, the corresponding TFC is increased to 967.031 \$/h, and the TVD takes the value 2.0747 p.u., this clearly proves the conflict aspect between the three objective functions.

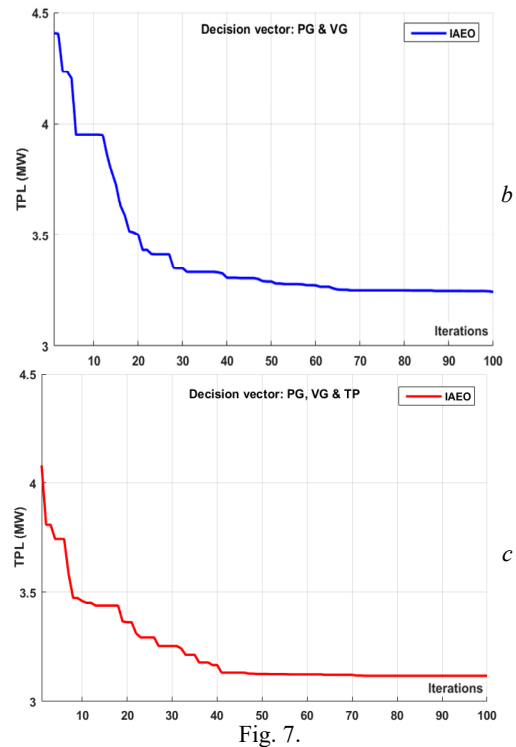
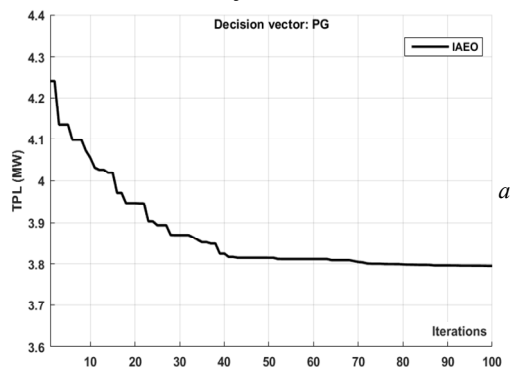


Fig. 7. *a* – convergence behavior of TFC minimization using IAEO at stage 1 (decision variables PG) for IEEE-30-Bus; *b* – convergence behavior of TFC minimization using IAEO at stage 2 (decision variables PG and VG) for IEEE-30-Bus; *c* – convergence behavior of TFC minimization using IAEO at stage 3 (decision variables PG, VG and TP) for IEEE-30-Bus

The convergence behavior of the TPL minimization at the final stage is shown in Fig. 8. The profile of voltage magnitudes obtained after optimization is shown in Fig. 11. It is clear that all the voltages at all PV and PQ-buses are within their permissible limits.

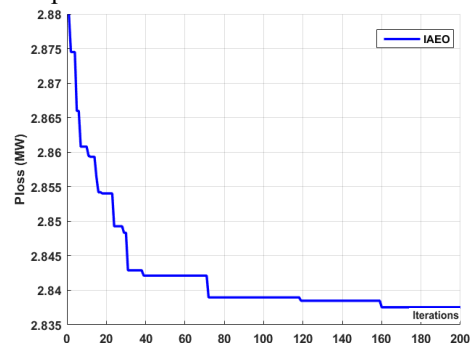


Fig. 8. Convergence behavior of TPL minimization using IAEO at the final stage for IEEE-30-Bus

Case-3: TVD improvement. The TVD is also an important index of power quality to evaluate the reliability of electric system. In this third case, the best TVD optimized at the final stage is improved to 0.1098 p.u., as a consequence the TFC is increased to 860.9828 \$/h, and the TPL is also increased to 6.9278 MW. This proves the conflict aspect between TVD minimization and other objective functions. The convergence characteristics of TVD improvement during the three successive stages are shown in Fig. 9,*a-c*.

The convergence behavior at the final stage is shown in Fig. 10. It is important to confirm that, all optimized results are found at a reduced number of iteration and trials.

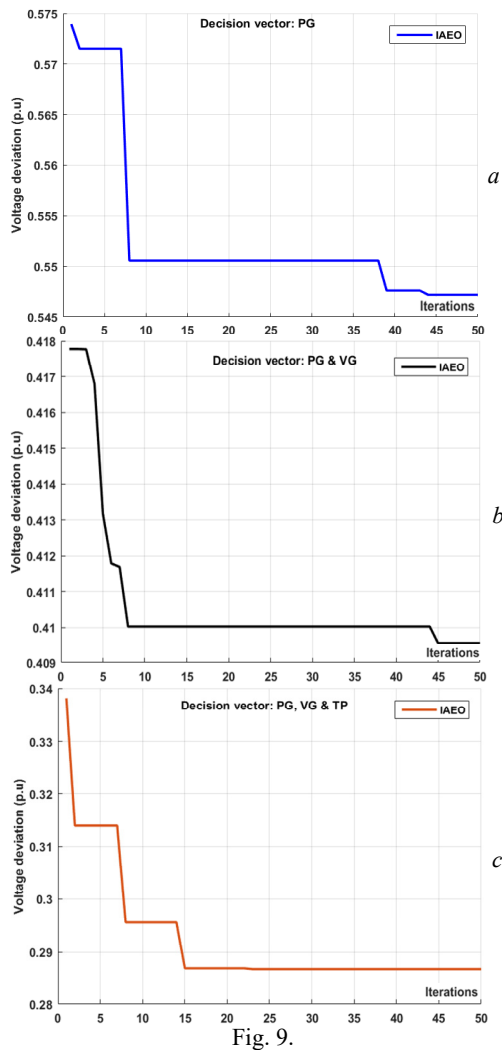


Fig. 9.

- a – convergence behavior of TVD minimization using IAEO at stage 1 (decision variables PG) for IEEE-30-Bus;
- b – convergence behavior of TVD minimization using IAEO at stage 2 (decision variables PG and VG) for IEEE-30-Bus;
- c – convergence behavior of TVD minimization using IAEO at stage 3 (decision variables PG, VG and TP) for IEEE-30-Bus

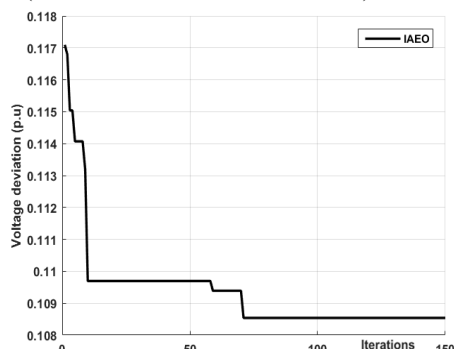


Fig. 10. Convergence behavior of TVD minimization using IAEO at the final stage for IEEE-30-Bus

The profiles of voltage magnitudes obtained after optimization are shown in Fig. 11.

Case-4: TFC and TPL improvement. Based on detailed results depicted in Table 1, it is confirmed that when optimizing individually each objective function, the optimized primary objective function will affect the quality of other objective functions. For this pertinent reason, and in this case, the TFC is improved in coordination with the TPL, this allows expert to identify an adequate compromise

solution based on specified technical and economic aspects. For this fourth case, the optimized TFC in coordination with TPL are 805.546 \$/h, and 6.9278 MW and consequently the TVD takes the value 1.8877 p.u.

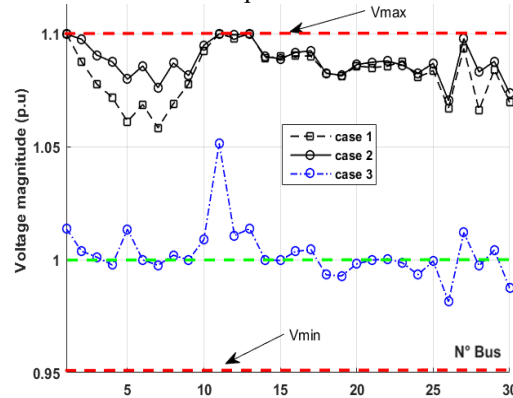


Fig. 11. The profiles of voltage magnitudes for cases: 1-2-3 for IEEE-30-Bus

Case-5: TPL and TVD improvement. One might think that improving the voltage magnitude will reduce the total power loss; this conclusion is relatively true when considering radial distribution system. However, in a meshed high transmission system, the improvement of TVD and TPL may be conflict. Also, it is important to optimize the TPL in coordination with TVD. For this case, the optimized values of TPL and TVD become 3.6426 MW and 0.1204 p.u., respectively, as a consequence the TFC achieves the value 964.2807 \$/h. As well shown in Table 3, it is important to confirm that there is no violation of constraints of reactive power associated to all generating units.

Case-6: TFC and TVD improvement. As well demonstrated in case 1 when the TFC is optimized at a competitive value (798.9457 \$/h), as a consequence the TVD takes high value (1.9582 p.u.). In this case, the main objective is to find a compromise solution between the TFC and the TVD which may be considered as an important issue for decision maker to ensure right equilibrium between economic and technical constraints imposed to utilities. Ensuring efficient TVD without affecting greatly the TFC has a positive impact on power quality. In this case, the optimized TVD is obtained by efficient coordination between the three suboptimal solutions found during the three stages associated to three decision variables. The best optimized TFC and TVD achieved at the last stage are 807.0926 \$/h and 0.1348 p.u., respectively. As well shown in Table 3, there is no violation of security limits associated to reactive power of thermal generating units.

Test-2: IEEE-57-bus. The efficiency and particularity of the proposed OPF management based IAEO is also validated on the IEEE-57-bus. Details technical data of the IEEE-57-bus in terms of cost coefficients, lines and buses data can be retrieved from [34]. The total apparent power to satisfy is $(1250.8 + j336.4)$ MVA, the maximum and minimum limits of tap setting transformers are in the limits [0.90, 1.1] in p.u., the permissible voltage limits of generating units are in the limits [0.95, 1.1] p.u., and the minimum and maximum bounds of PQ buses are taken in the limits [0.95, 1.1] p.u., however for fair comparison with other techniques, the security limits of voltage magnitudes at PQ buses are also considered to be in the limits [0.95, 1.05]. The IEEE-57-bus electric network consists of a

total of 34 decision variables, including 14 variables related to PV buses, 17 tap transformers, and 3 capacitor banks. In this study three SVC devices are used. To improve the

solution quality of the various OPF problems, three objective functions have been optimized such as the TFC, the TPL and the TVD.

Table 3

Values of reactive power of generating units after optimization: cases 1 to 6

State variables, MVar	Q_{Gmin} , MVar	Q_{Gmax} , MVar	Case-1	Case-2	Case-3	Case-4	Case-5	Case-6
Q_{G1}	-20	200	-16.4008	-10.0181	-20.0000	-10.5765	-3.0497	-20.0000
Q_{G2}	-20	100	21.7922	8.3262	-3.5263	16.4079	-20.0000	-6.5415
Q_{G5}	-15	80	26.6227	21.9110	49.0411	24.4629	45.8506	57.9317
Q_{G8}	-15	60	31.5658	31.0241	35.4018	28.4477	27.4492	41.6220
Q_{G11}	-10	50	11.8436	10.5031	26.7630	12.9860	27.4764	26.9296
Q_{G13}	-15	60	1.6210	1.1132	2.3241	2.9223	1.9628	2.7053

Case-7: TFC improvement. For this case, two scenarios are considered. In the first scenario, the security limits of voltages of generators are taken in the limits [0.95, 1.1], the optimized TFC achieved is 41638.6742 (\$/h) which is better compared to the results found from other recent methods such as: Improved Chaotic Electromagnetic Field optimization (ICEFO), Electromagnetic Field Optimization (EFO), PSO, BBO, DE, and ABC. In the second scenario and for fair comparison with other techniques, the TFC is optimized by considering the voltage

magnitudes limits in the limits [0.95, 1.05]. For this second scenario the optimized TFC is increased to 41684.00 \$/h due to the new voltage constraints associated to PQ buses. Table 4 shows the optimized control variables using the proposed IAEO approach. Figure 12 shows the convergence of TFC minimization using IAEO at the final stage. The distributions of voltage magnitudes of TFC minimization for two scenarios are shown in Fig. 13. It is also important to confirm that all security constraints are satisfied.

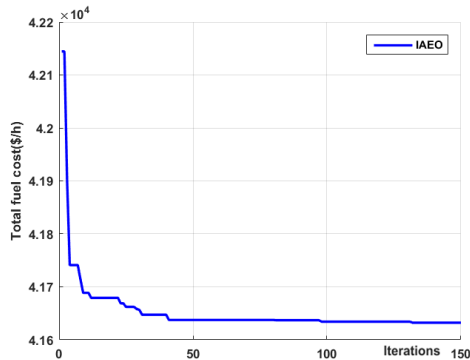


Fig. 12. Convergence behavior of TFC improvement using IAEO at the final stage for IEEE-57-bus electric system

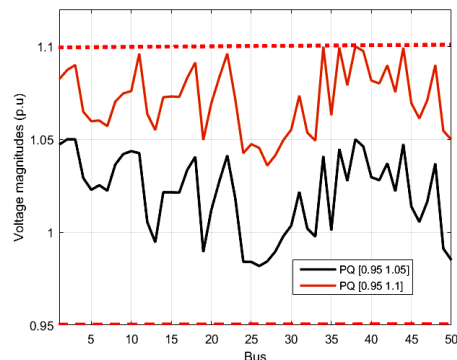


Fig. 13. The voltage profiles of IEEE-57-bus for TFC improvement

Table 4

Optimized decision variables for TFC minimization: Test-system-2: IEEE-57-bus: case-7

Control variables	Min	Scenario 1	Scenario 2	Max	Control variables	Min	Scenario 1	Scenario 2	Max
Pg1	0	142.4616	142.8434	575.88	T24-25	0.9	1.0926	1.0947	1.1
Pg2	0	87.8254	90.4059	100.00	T24-26	0.9	1.0229	1.0432	1.1
Pg3	0	44.7744	45.0471	140.00	T7-29	0.9	0.9837	1.0042	1.1
Pg6	0	72.1854	71.4206	100.00	T34-32	0.9	0.9598	0.9805	1.1
Pg8	0	461.9187	459.2815	550.00	T11-41	0.9	0.9072	0.9182	1.1
Pg9	0	96.5357	96.4080	100.00	T15-45	0.9	0.9621	0.9828	1.1
Pg12	0	359.3850	360.6297	410.00	T14-46	0.9	0.9481	0.9688	1.1
Vg1	0.95	1.0742	1.0588	1.1	T10-51	0.9	0.9567	0.9774	1.1
Vg2	0.95	1.0708	1.0566	1.1	T13-49	0.9	0.9207	0.9416	1.1
Vg3	0.95	1.0600	1.0496	1.1	T11-43	0.9	0.9549	0.9756	1.1
Vg6	0.95	1.0821	1.0565	1.1	T40-56	0.9	0.9910	1.0115	1.1
Vg8	0.95	1.1000	1.0600	1.1	T39-57	0.9	0.9607	0.9814	1.1
Vg9	0.95	1.0696	1.0373	1.1	T9-55	0.9	0.9744	0.9950	1.1
Vg12	0.95	1.0650	1.0429	1.1	Q_{SVC18} (MVar)	0	6.0099	5.2929	20
T4-18	0.9	0.9530	0.9737	1.1	Q_{SVC25} (MVar)	0	14.3869	15.7339	20
T4-18	0.9	0.9792	0.9998	1.1	Q_{SVC53} (MVar)	0	11.7961	12.5047	20
T21-20	0.9	1.0094	1.0298	1.1					
T24-25	0.9	0.9628	0.9835	1.1					
TFC, \$/h		41638.6742	41684.00						
TPL, MW		14.2861	15.2362						
TVD, p.u.		3.3403	1.2506						
Voltage of PQ bus limits, p.u.		[0.95, 1.1]	[0.95, 1.05]				[0.95, 1.1]	[0.95, 1.05]	

Case-8: TPL improvement. Two scenarios are considered to improve the TPL. In the first scenario and by considering the limits of voltages of PQ buses in the limits [0.95, 1.1] p.u., the best TPL found using IAEO is 9.288 MW which is better compared to results found from others techniques [18]. However, in the second scenario, when the margin security of voltages of PQ buses are [0.95 1.05] p.u., the TPL achieved becomes 10.1677 MW. The values of optimized decision variables such as real power and voltage magnitudes of generators, tap

transformers, and reactive power of SVC devices installed at buses (18, 25, and 53) are depicted in Table 5.

The convergence behavior of TPL improvement in the last stage for scenario 1 is shown in Fig. 14. The profile of voltages at all PQ-buses for the two permissible voltage magnitude limits [0.95, 1.1] p.u. and [0.95, 1.05] p.u. are shown in Fig 15. It is clear that the proposed IAEO gives better results in terms of solution quality and also convergence behaviours.

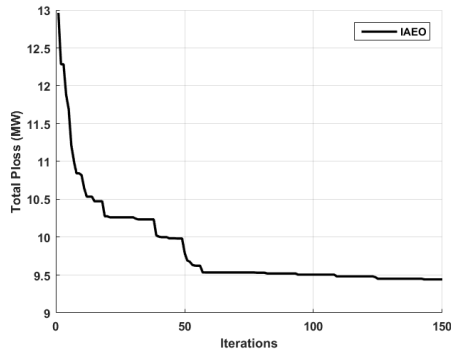


Fig. 14. Convergence behavior of TPL improvement using IAEO at the final stage for IEEE-57-bus electric system

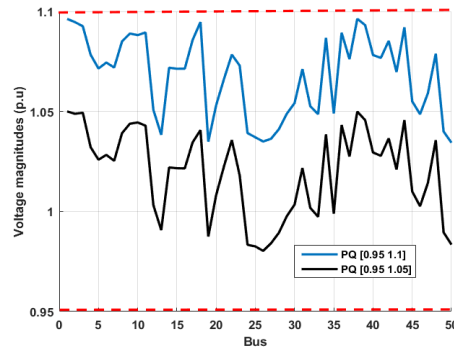


Fig. 15. The profile of voltages for IEEE-57-bus for TPL minimization

Table 5

Optimized decision variables for Test-system-2: IEEE-57-bus: case-8

Decision variables	Min	Scenario 1	Scenario 2	Max	Control variables	Min	Scenario 1	Scenario 2	Max
Pg1	0	199.0713	200.5999	575.88	T24-25	0.9	1.1000	1.0988	1.1
Pg2	0	4.236000	2.5244	100.00	T24-26	0.9	1.0485	1.0473	1.1
Pg3	0	139.3166	139.2099	140.00	T7-29	0.9	1.0095	1.0083	1.1
Pg6	0	99.99220	99.9989	100.00	T34-32	0.9	0.9858	0.9846	1.1
Pg8	0	307.4738	308.6348	550.00	T11-41	0.9	0.9235	0.9223	1.1
Pg9	0	99.99910	99.9998	100.00	T15-45	0.9	0.9881	0.9869	1.1
Pg12	0	409.9993	409.9999	410.00	T14-46	0.9	0.9741	0.9729	1.1
Vg1	0.95	1.1000	1.0587	1.1	T10-51	0.9	0.9827	0.9815	1.1
Vg2	0.95	1.0953	1.0523	1.1	T13-49	0.9	0.9469	0.9457	1.1
Vg3	0.95	1.1000	1.0539	1.1	T11-43	0.9	0.9809	0.9797	1.1
Vg6	0.95	1.0985	1.0532	1.1	T40-56	0.9	1.0168	1.0156	1.1
Vg8	0.95	1.1000	1.0600	1.1	T39-57	0.9	0.9867	0.9855	1.1
Vg9	0.95	1.0836	1.0397	1.1	T9-55	0.9	1.0003	0.9991	1.1
Vg12	0.95	1.0913	1.0454	1.1	Q _{SVC18} (MVar)	0	5.8044	6.0732	20
T4-18	0.9	0.9790	0.9778	1.1	Q _{SVC25} (MVar)	0	16.2454	16.5142	20
T4-18	0.9	1.0051	1.0039	1.1	Q _{SVC53} (MVar)	0	13.0162	13.2850	20
T21-20	0.9	1.0351	1.0339	1.1					
T24-25	0.9	0.9888	0.9876	1.1					
TFC, \$/h		44936.637	44976.00						
TPL, MW		9.2880	10.1677						
TVD, p.u.		3.3893	1.2496						
Voltage of PQ bus limits, p.u.		[0.95, 1.1]	[0.95, 1.05]				[0.95, 1.1]	[0.95, 1.05]	

Case-9: TVD improvement. As well shown in results found for TFC minimization, the TVD increases to a high value p.u., this confirms the conflict behaviour between TFC and TVD. For this case, the TVD is optimized individually, the optimized value of TVD achieved is 0.7613 p.u., as a consequence, the TFC and the TPL become, 43637.599 \$/h, 12.6659 MW respectively. The convergence behavior of TVD minimization is shown in Fig. 16. The optimized decision variables are shown in Table 6. All security constraints are in their admissible bounds.

Table 7 shows detailed results related for generated reactive power for cases 7, 8, 9.

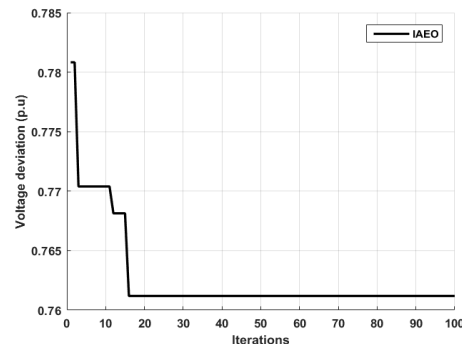


Fig. 16. Convergence behavior of TVD improvement using IAEO at the final stage for IEEE-57-bus electric network

Optimized decision variables for Test-system 2: IEEE-57-bus: case-9

Decision variables	Min	Optimized	Max	Decision variables	Min	Optimized	Max
Pg1	0	253.2690	575.88	T24-25	0.9	1.0802	1.1
Pg2	0	35.1258	100.00	T24-26	0.9	1.0223	1.1
Pg3	0	84.8772	140.00	T7-29	0.9	0.9833	1.1
Pg6	0	69.7737	100.00	T34-32	0.9	0.9596	1.1
Pg8	0	333.2967	550.00	T11-41	0.9	0.9173	1.1
Pg9	0	91.3378	100.00	T15-45	0.9	0.9619	1.1
Pg12	0	395.7857	410.00	T14-46	0.9	0.9479	1.1
Vg1	0.95	1.0266	1.1	T10-51	0.9	0.9565	1.1
Vg2	0.95	1.0148	1.1	T13-49	0.9	0.9207	1.1
Vg3	0.95	1.0095	1.1	T11-43	0.9	0.9547	1.1
Vg6	0.95	1.0061	1.1	T40-56	0.9	0.9906	1.1
Vg8	0.95	1.0079	1.1	T39-57	0.9	0.9605	1.1
Vg9	0.95	0.9920	1.1	T9-55	0.9	0.9741	1.1
Vg12	0.95	1.0111	1.1	Q _{SVC18} (MVar)	0	8.6025	20
T4-18	0.9	0.9528	1.1	Q _{SVC25} (MVar)	0	19.2413	20
T4-18	0.9	0.9789	1.1	Q _{SVC53} (MVar)	0	15.9510	20
T21-20	0.9	1.0089	1.1		-		
T24-25	0.9	0.9626	1.1				
TFC, \$/h	43637.599						
TPL, MW	12.6659						
TVD, p.u.	0.7613						
Voltage of PQ bus limits, p.u.	[0.95, 1.1]						

Table 7

Values of reactive power of generating units after optimization: cases 7, 8, 9, for IEEE-57-bus electric system

State variables, MVar	Q _{Gmin} , MVar	Q _{Gmax} , MVar	Case-7	Case-8	Case-9
Q _{G1}	-140	200	41.2497	25.1539	63.2333
Q _{G2}	-17	50	50.0000	50.0000	29.6884
Q _{G3}	-10	60	33.7970	30.6423	29.1474
Q _{G6}	-8	25	11.9570	-0.0081	5.3507
Q _{G8}	-140	200	31.8761	34.7790	27.0905
Q _{G9}	-3	9	8.7930	9.0000	3.8068
Q _{G12}	-150	155	55.4596	52.0659	73.4293

Comparative study and robustness evaluation. A

comparative analysis is introduced to validate the performances and particularity of the proposed approach based IAEO designed to solve multi objective OPF. In the recent literature many several metaheuristic methods have been proposed to improve the solution quality of various OPF problems. It is found that some comparative studies are not adequate for one reason; the security limits associated to voltage of PQ-buses are not similar. In order to relieve conflicts about this subject, in this study, the OPF problem with various objective functions have been solved considering three types of constraints related to the voltage magnitudes of PQ-buses. In the first scenario, the security limits of voltage magnitudes of PQ-buses are taken in the limits [0.95, 1.1] p.u., in the second scenario, the admissible bounds of voltage magnitudes of PQ-buses are considered in the limits [0.95, 1.05] p.u., and in the third scenario the limits of voltage magnitudes of PQ-buses are taken in the limits [0.94, 1.06] p.u.. Table 8 shows a comparative analysis of statistical results for TFC, TPL and TVD minimization using the proposed method and other recent methods. The optimized results related to the first scenario are depicted in Table 6. These values are achieved by considering the voltage magnitudes of PQ buses in the limits [0.95, 1.1]. It is well demonstrated, that the proposed

IAEO converges to a competitive value of TFC (41,638.6742 \$/h) compared to other methods, expect the value of TFC achieved using the APFPA [18], otherwise, the TPL and TVD are also improved to a complete values, 9.28 MW, 0.7613 p.u., respectively.

Table 8

Comparative study: best results for TFC, TPL and TVD improvement for test system IEEE-57-bus: voltage magnitude at PQ-buses is in the limits [0.95, 1.1] p.u.

Methods: [6, 18, 20]	TFC, \$/h	TPL, MW	TVD, p.u.
ICEFO	41,706.1117	-	-
EFO	41,706.3467	-	-
PSO	42,386.3675	-	-
BBO	41,698.9307	-	-
DE	41,689.7303	-	-
ABC	41,715.7607	-	-
APFPA	41,628.7520	9.3151	0.8909
CSSO	41,666.6620	-	-
Proposed method IAEO	41,638.6742	9.2800	0.7613

The results of the OPF for the second and third scenario are depicted in Table 9.

Table 9

Comparative study: best results for TFC, TPL and TVD improvement for electric system IEEE-57-bus: voltage magnitude at PQ-buses is in the limits [0.95, 1.05] p.u.

Methods [14, 21]	TFC, \$/h	TPL, MW	TVD, p.u.	Observations
TLBO	41,688.7431	-	-	[0.95 1.05]
MTLBO	41,638.3822*	-	-	[0.95 1.05]
SKH	41,676.9152	10.6877	-	[0.94 1.06]
KH	41,681.3521	11.2158	-	[0.94 1.06]
Proposed method IAEO	41,684.0000	10.1677	0.7613	[0.95 1.05]
	41,668.3663	9.9827	-	[0.94 1.06]

* Infeasible solution

The best TFC achieved using the proposed IAEO is compared to the results achieved using TLBO [14], MTLBO

[14], stud krill herd (SKH) algorithm [21], and the standard krill herd (KH) algorithm [21]. It is observed that the proposed IAEO algorithm achieves better optimal values compared to other methods, except the TFC achieved using MTLBO (41,638.3822 \$/h), however, after verification by using the power flow tool, it is found that the obtained results are not feasible, violations of constraints in term of voltage magnitudes in several PQ buses. The proposed method

named IAEO achieves better optimal TFC (41,668.3663 \$/h) by considering the voltage magnitudes of PQ buses in the limits [0.94, 1.06] p.u., and by considering the voltage magnitudes of PQ buses in the limits [0.95, 1.05], the new optimized TFC values becomes 41,686.00 \$/h. Tables 10, 11 show the optimal settings of decision variables achieved for TFC minimization and TPL improvement using the proposed IAEO method and the SKH method [14, 21].

Table 10

Optimal settings of decision variables of TFC minimization for Test-system-2: IEEE-57-bus: PQ-buses [0.94, 1.06] p.u.

Control variables	Min	IAEO	SKH [21]	Max	Control variables	Min	IAEO	SKH [21]	Max
Pg1	0	142.6746	142.8235	575.88	T24-25	0.9	1.0816	1.0782	1.1
Pg2	0	89.32490	90.4827	100.00	T24-26	0.9	1.0345	1.0257	1.1
Pg3	0	44.99740	45.1846	140.00	T7-29	0.9	0.9953	0.9895	1.1
Pg6	0	71.49150	71.8808	100.00	T34-32	0.9	0.9714	0.9691	1.1
Pg8	0	460.6816	459.2338	550.00	T11-41	0.9	0.9088	0.9008	1.1
Pg9	0	96.39720	96.1160	100.00	T15-45	0.9	0.9737	0.9740	1.1
Pg12	0	360.1558	360.1577	410.00	T14-46	0.9	0.9597	0.9591	1.1
Vg1	0.95	1.0570	1.0593	1.1	T10-51	0.9	0.9683	0.9649	1.1
Vg2	0.95	1.0551	1.0575	1.1	T13-49	0.9	0.9323	0.9310	1.1
Vg3	0.95	1.0489	1.0512	1.1	T11-43	0.9	0.9665	0.9657	1.1
Vg6	0.95	1.0595	1.0594	1.1	T40-56	0.9	1.0026	0.9937	1.1
Vg8	0.95	1.0747	1.0599	1.1	T39-57	0.9	0.9723	0.9629	1.1
Vg9	0.95	1.0451	1.0373	1.1	T9-55	0.9	0.9860	0.9846	1.1
Vg12	0.95	1.0414	1.0416	1.1	Q _{SVC18} , MVar	0	5.6309	0.1580	20
T4-18	0.9	0.9646	0.9062	1.1	Q _{SVC25} , MVar	0	14.0079	0.1563	20
T4-18	0.9	0.9908	1.0955	1.1	Q _{SVC53} , MVar	0	11.4171	0.1380	20
T21-20	0.9	1.0210	1.0106	1.1					
T24-25	0.9	0.9744	0.9815	1.1					
TFC, \$/h		41,668.391696	41,676.9152						
TPL, MW		14.923	15.0795						
TVD, p.u.		1.5901	-						
Voltage of PQ buses limits, p.u.	[0.94, 1.06]								

Table 11

Optimal settings of decision variables of TPL minimization for Test-system-2: IEEE-57-bus: PQ-buses [0.94, 1.06] p.u.

Control variables	Min	IAEO	SKH [21]	Max	Control variables	Min	IAEO	SKH [21]	Max
Pg1	0	203.4968	200.9220	575.88	T24-25	0.9	1.0823	1.0312	1.1
Pg2	0	2.282400	3.3270	100.00	T24-26	0.9	1.0508	1.0021	1.1
Pg3	0	137.2892	139.9317	140.00	T7-29	0.9	1.0118	0.9327	1.1
Pg6	0	99.99880	99.9470	100.00	T34-32	0.9	0.9881	0.9493	1.1
Pg8	0	307.7157	307.3602	550.00	T11-41	0.9	0.9258	0.9004	1.1
Pg9	0	99.99990	100.0000	100.00	T15-45	0.9	0.9904	0.9176	1.1
Pg12	0	409.9999	409.9996	410.00	T14-46	0.9	0.9764	0.9059	1.1
Vg1	0.95	1.0732	1.0023	1.1	T10-51	0.9	0.9850	0.9172	1.1
Vg2	0.95	1.0658	0.9957	1.1	T13-49	0.9	0.9492	0.9001	1.1
Vg3	0.95	1.0642	0.9987	1.1	T11-43	0.9	0.9832	0.9026	1.1
Vg6	0.95	1.0623	0.9983	1.1	T40-56	0.9	1.0191	1.0000	1.1
Vg8	0.95	1.0713	1.0012	1.1	T39-57	0.9	0.9890	0.9776	1.1
Vg9	0.95	1.0528	0.9795	1.1	T9-55	0.9	1.0026	0.9263	1.1
Vg12	0.95	1.0610	0.9855	1.1	Q _{SVC18} , MVar	0	5.9720	0.0605	20
T4-18	0.9	0.9813	0.9643	1.1	Q _{SVC25} , MVar	0	16.4130	0.1399	20
T4-18	0.9	1.0074	0.9004	1.1	Q _{SVC53} , MVar	0	13.1838	0.1262	20
T21-20	0.9	1.0374	1.0096	1.1					
T24-25	0.9	0.9911	0.9759	1.1					
TFC, \$/h		44,912.826117	45,044.2407						
TPL, MW		9.9827	10.6877						
TVD, p.u.		1.6011	-						
Voltage of PQ bus limits, p.u.	[0.94, 1.06]								

Robustness evaluation. The efficiency of the proposed variant namely IAEO has been validated on two practical electric systems, the IEEE-30-bus, and the

IEEE-57-bus considering various objective functions. Compared to the standard algorithm (AEO), the proposed variant needs a reduced number of generations and trials

to converge to the best solution (100 to 150 generations, and between 5 to 10 trials). Also, due to the interactive decomposed concept based on optimizing a reduced number of decision variables, the proposed variant needs a small number of population and a reduced number of trials to explore the global search space. As well demonstrated on results given, the maximum number of iteration and population required to optimize all subsystems are 50 and 10, respectively. However in the last stage and to ensure fine intensification around the near optimal solution, the number of iteration required is relatively increased to 150.

Conclusion. This paper is elaborated to apply an efficient Interactive Artificial Ecosystem Algorithm (IAEO) to improve the solution quality of the multi objective OPF problem. Three objective functions such as the TFC, TPL and TVD have been optimized individually and simultaneously to improve the performances of practical power systems considering the integration of multi SVC based FACTS devices. For the IEEE 30-Bus test system, the optimized values for TFC, TPL and TVD are 798.9457 \$/h, 2.83530 MW and 0.10980 p.u., respectively, and for the test system IEEE 57-Bus, the best values achieved for TFC, TPL and TVD are 41,638.6742 \$/h, 9.28 MW and 0.7613 p.u., respectively. The mechanism search of the standard AEO is improved by creating flexible interactivity during search process between intensification and diversification. Initially, a specified number of sub systems have been created based on the types of decision variables. This first stage allows creating diversity in search space, and then at the final stages, the search process is guided to achieve an efficient local search around the best updated solution. The performances of the proposed optimization technique have been validated on two practical IEEE test systems. The obtained results using the proposed IAEO compared to many recent methods demonstrate its efficiency and competitive aspect in solving power management optimization.

Conflict of interest. The authors declare no conflict of interest.

REFERENCES

1. Carpentier J. Contribution à l'étude du dispatching économique. *Bulletin de la Société Française des électriciens*, 1962, vol. 3, pp. 431-447. (Fra).
2. Ullah Z., Elkadeem M.R., Wang S., Azam M., Shaheen K., Hussain M., Rizwan M. A Mini-review: Conventional and Metaheuristic Optimization Methods for the Solution of Optimal Power Flow (OPF) Problem. In: Barolli, L., Amato, F., Moscato, F., Enokido, T., Takizawa, M. (eds) *Advanced Information Networking and Applications. AINA 2020. Advances in Intelligent Systems and Computing*, 2020, vol. 1151. Springer, Cham. doi: https://doi.org/10.1007/978-3-030-44041-1_29.
3. Frank S., Steponavice I., Rebennack S. Optimal power flow: a bibliographic survey II. *Energy Systems*, 2012, vol. 3, no. 3, pp. 259-289. doi: <https://doi.org/10.1007/s12667-012-0057-x>.
4. Mahdad B., Srairi K. A new interactive sine cosine algorithm for loading margin stability improvement under contingency. *Electrical Engineering*, 2018, vol. 100, no. 2, pp. 913-933. doi: <https://doi.org/10.1007/s00202-017-0539-x>.
5. Mahdad B. Improvement optimal power flow solution under loading margin stability using new partitioning whale algorithm. *International Journal of Management Science and Engineering Management*, 2019, vol. 14, no. 1, pp. 64-77. doi: <https://doi.org/10.1080/17509653.2018.1488225>.

6. Bouchekara H. Solution of the optimal power flow problem considering security constraints using an improved chaotic electromagnetic field optimization algorithm. *Neural Computing and Applications*, 2020, vol. 32, no. 7, pp. 2683-2703. doi: <https://doi.org/10.1007/s00521-019-04298-3>.
7. Kotb M.F., El-Fergany A.A. Optimal Power Flow Solution Using Moth Swarm Optimizer Considering Generating Units Prohibited Zones and Valve Ripples. *Journal of Electrical Engineering & Technology*, 2019, vol. 15, pp. 179-192. doi: <https://doi.org/10.1007/s42835-019-00144-7>.
8. Taher M.A., Kamel S., Jurado F., Ebeed M. Modified grasshopper optimization framework for optimal power flow solution. *Electrical Engineering*, 2019, vol. 101, no. 1, pp. 121-148. doi: <https://doi.org/10.1007/s00202-019-00762-4>.
9. Warid W. Optimal power flow using the AMTPG-Jaya algorithm. *Applied Soft Computing*, 2020, vol. 91, art. no. 106252. doi: <https://doi.org/10.1016/j.asoc.2020.106252>.
10. El-Fergany A.A., Hasanien H.M. Tree-seed algorithm for solving optimal power flow problem in large-scale power systems incorporating validations and comparisons. *Applied Soft Computing*, 2018, vol. 64, pp. 307-316. doi: <https://doi.org/10.1016/j.asoc.2017.12.026>.
11. Radosavljević J., Klimenta D., Jevtić M., Arsić N. Optimal Power Flow Using a Hybrid Optimization Algorithm of Particle Swarm Optimization and Gravitational Search Algorithm. *Electric Power Components and Systems*, 2015, vol. 43, no. 17, pp. 1958-1970. doi: <https://doi.org/10.1080/15325008.2015.1061620>.
12. Youssef H., Kamel S., Ebeed, M. Optimal Power Flow Considering Loading Margin Stability Using Lightning Attachment Optimization Technique. *2018 Twentieth International Middle East Power Systems Conference (MEPCON)*, 2018, pp. 1053-1058. doi: <https://doi.org/10.1109/MEPCON.2018.8635110>.
13. Berrouk F., Bounaya K. Optimal Power Flow For Multi-FACTS Power System Using Hybrid PSO-PS Algorithms. *Journal of Control, Automation and Electrical Systems*, 2018, vol. 29, no. 2, pp. 177-191. doi: <https://doi.org/10.1007/s40313-017-0362-7>.
14. Shabanpour-Haghighi A., Seifi A.R., Niknam T. A modified teaching-learning based optimization for multi-objective optimal power flow problem. *Energy Conversion and Management*, 2014, vol. 77, pp. 597-607. doi: <https://doi.org/10.1016/j.enconman.2013.09.028>.
15. Mugemanyi S., Qu Z., Rugema F.X., Dong Y., Bananeza C., Wang L. Optimal Reactive Power Dispatch Using Chaotic Bat Algorithm. *IEEE Access*, 2020, vol. 8, pp. 65830-65867. doi: <https://doi.org/10.1109/ACCESS.2020.2982988>.
16. Nguyen T.T. A high performance social spider optimization algorithm for optimal power flow solution with single objective optimization. *Energy*, 2019, vol. 171, pp. 218-240. doi: <https://doi.org/10.1016/j.energy.2019.01.021>.
17. Kahourzade S., Mahmoudi A., Mokhlis H. Bin. A comparative study of multi-objective optimal power flow based on particle swarm, evolutionary programming, and genetic algorithm. *Electrical Engineering*, 2015, vol. 97, no. 1, pp. 1-12. doi: <https://doi.org/10.1007/s00202-014-0307-0>.
18. Mahdad B., Srairi K. Security constrained optimal power flow solution using new adaptive partitioning flower pollination algorithm. *Applied Soft Computing*, 2016, vol. 46, pp. 501-522. doi: <https://doi.org/10.1016/j.asoc.2016.05.027>.
19. Mahdad B., Kamel S. New strategy based modified Salp swarm algorithm for optimal reactive power planning: a case study of the Algerian electrical system (114 bus). *IET Generation, Transmission & Distribution*, 2019, vol. 13, no. 20, pp. 4523-4540. doi: <https://doi.org/10.1049/iet-gtd.2018.5772>.
20. Bentouati B., Javaid M.S., Bouchekara H.R.E.H., El-Fergany A.A. Optimizing performance attributes of electric power systems using chaotic Salp swarm optimizer. *International Journal of Management Science and Engineering*

- Management*, 2020, vol. 15, no. 3, pp. 165-175. doi: <https://doi.org/10.1080/17509653.2019.1677197>.
21. Pulluri H., Naresh R., Sharma V. A solution network based on stud krill herd algorithm for optimal power flow problems. *Soft Computing*, 2018, vol. 22, no. 1, pp. 159-176. doi: <https://doi.org/10.1007/s00500-016-2319-3>.
22. Li S., Gong W., Wang L., Yan X., Hu C. Optimal power flow by means of improved adaptive differential evolution. *Energy*, 2020, vol. 198, art. no. 117314. doi: <https://doi.org/10.1016/j.energy.2020.117314>.
23. El-Fergany A.A., Hasanien H.M. Salp swarm optimizer to solve optimal power flow comprising voltage stability analysis. *Neural Computing and Applications*, 2020, vol. 32, no. 9, pp. 5267-5283. doi: <https://doi.org/10.1007/s00521-019-04029-8>.
24. Sakthivel V.P., Suman M., Sathya P.D. Squirrel search algorithm for economic dispatch with valve-point effects and multiple fuels. *Energy Sources, Part B: Economics, Planning, and Policy*, 2020, vol. 15, no. 6, pp. 351-382. doi: <https://doi.org/10.1080/15567249.2020.1803451>.
25. Meng A., Zeng C., Wang P., Chen D., Zhou T., Zheng X., Yin H. A high-performance crisscross search based grey wolf optimizer for solving optimal power flow problem. *Energy*, 2021, vol. 225, art. no. 120211. doi: <https://doi.org/10.1016/j.energy.2021.120211>.
26. Mehdi M.F., Ahmad A., Ul Haq S.S., Saqib M., Ullah M.F. Dynamic economic emission dispatch using whale optimization algorithm for multi-objective function. *Electrical Engineering & Electromechanics*, 2021, no. 2, pp. 64-69. doi: <https://doi.org/10.20998/2074-272X.2021.2.09>.
27. Kouadri R., Slimani L., Bouktir T. Slime mould algorithm for practical optimal power flow solutions incorporating stochastic wind power and static var compensator device. *Electrical Engineering & Electromechanics*, 2020, no. 6, pp. 45-54. doi: <https://doi.org/10.20998/2074-272X.2020.6.07>.
28. Djabali C., Bouktir T. Simultaneous allocation of multiple distributed generation and capacitors in radial network using genetic-salp swarm algorithm. *Electrical Engineering & Electromechanics*, 2020, no. 4, pp. 59-66. doi: <https://doi.org/10.20998/2074-272X.2020.4.08>.
29. Zhao W., Wang L., Zhang Z. Artificial ecosystem-based optimization: a novel nature-inspired meta-heuristic algorithm. *Neural Computing and Applications*, 2020, vol. 32, no. 13, pp. 9383-9425. doi: <https://doi.org/10.1007/s00521-019-04452-x>.
30. Mouassa S., Jurado F., Bouktir T., Raja M.A.Z. Novel design of artificial ecosystem optimizer for large-scale optimal reactive power dispatch problem with application to Algerian electricity grid. *Neural Computing and Applications*, 2021, vol. 33, no. 13, pp. 7467-7490. doi: <https://doi.org/10.1007/s00521-020-05496-0>.
31. Shaheen A., Elsayed A., Ginidi A., El-Sehiemy R., Elattar E. Reconfiguration of electrical distribution network-based DG and capacitors allocations using artificial ecosystem optimizer: Practical case study. *Alexandria Engineering Journal*, 2022, vol. 61, no. 8, pp. 6105-6118. doi: <https://doi.org/10.1016/j.aej.2021.11.035>.
32. Khasanov M., Kamel S., Tostado-Veliz M., Jurado F. Allocation of Photovoltaic and Wind Turbine Based DG Units Using Artificial Ecosystem-based Optimization. *2020 IEEE International Conference on Environment and Electrical Engineering and 2020 IEEE Industrial and Commercial Power Systems Europe (EEEIC / I&CPS Europe)*, 2020, pp. 1-5. doi: <https://doi.org/10.1109/EEEIC/ICPSEurope49358.2020.9160696>.
33. Eid A., Kamel S., Korashy A., Khurshaid T. An Enhanced Artificial Ecosystem-Based Optimization for Optimal Allocation of Multiple Distributed Generations. *IEEE Access*, 2020, vol. 8, pp. 178493-178513. doi: <https://doi.org/10.1109/ACCESS.2020.3027654>.
34. Zimmerman R.D., Murillo-Sanchez C.E., Thomas R.J. MATPOWER: Steady-State Operations, Planning, and Analysis Tools for Power Systems Research and Education. *IEEE Transactions on Power Systems*, 2011, vol. 26, no. 1, pp. 12-19. doi: <https://doi.org/10.1109/TPWRS.2010.2051168>.

Received 30.04.2022

Accepted 14.08.2022

Published 06.11.2022

Belkacem Mahdad¹, PhD,

Kamel Srairi¹, PhD,

¹University of Biskra, Algeria,

e-mail: Belkacem.mahdad@univ-biskra.dz (Corresponding Author);

k.srairi@univ-biskra.dz

How to cite this article:

Mahdad B., Srairi K. Interactive artificial ecosystem algorithm for solving power management optimizations. *Electrical Engineering & Electromechanics*, 2022, no. 6, pp. 53-66. doi: <https://doi.org/10.20998/2074-272X.2022.6.09>